Bioorganic & Medicinal Chemistry Letters 24 (2014) 3826–3834

Contents lists available at ScienceDirect

Bioorganic & Medicinal Chemistry Letters

journal homepage: www.elsevier.com/locate/bmcl

Inhibition of prostaglandin E_2 production by synthetic minor prenylated chalcones and flavonoids: Synthesis, biological activity, crystal structure, and in silico evaluation

Kamal Rullah [a,f], Mohd Fadhlizil Fasihi Mohd Aluwi [a], Bohari M. Yamin [b], Mohd Nazri Abdul Bahari [c], Leong Sze Wei [d], Syahida Ahmad [c], Faridah Abas [d], Nor Hadiani Ismail [e], Ibrahim Jantan [a], Lam Kok Wai [a,*]

[a] Drugs and Herbal Research Centre, Faculty of Pharmacy, Universiti Kebangsaan Malaysia, Jalan Raja Muda Abdul Aziz, 50300 Kuala Lumpur, Malaysia
[b] School of Chemical Sciences and Food Technology, Universiti Kebangsaan Malaysia, 43600 Bangi, Selangor, Malaysia
[c] Faculty of Biotechnology and Biomolecular Sciences, Universiti Putra Malaysia, 43400 Serdang, Selangor, Malaysia
[d] Institute of Bioscience, Universiti Putra Malaysia, 43400 Serdang, Selangor, Malaysia
[e] Faculty of Science, Universiti Teknologi MARA, 50400 Shah Alam, Selangor, Malaysia
[f] Sekolah Tinggi Ilmu Farmasi Riau, Universitas Riau, Kampus Bina Widya Km 12.5, Simpang baru-Pekanbaru, Indonesia

ARTICLE INFO

Article history:
Received 25 April 2014
Revised 11 June 2014
Accepted 20 June 2014
Available online 27 June 2014

Keywords:
Prenylated chalcone
Minor flavonoids
Single-crystal XRD
Prostaglandin E_2
COX-2 inhibitor
ADMET prediction

ABSTRACT

The discovery of potent inhibitors of prostaglandin E_2 (PGE_2) synthesis in recent years has been proven to be an important game changer in pharmaceutical industry. It is known that excessive production of PGE_2 triggers a vast array of biological signals and physiological events that contributes to inflammatory diseases such as rheumatoid arthritis, atherosclerosis, cancer, and pain. In this Letter, we report the synthesis of a series of minor prenylated chalcones and flavonoids which was found to be significantly active in suppressing the PGE_2 production secreted by lipopolysaccharide-induced mouse macrophage cells (RAW 264.7). Among the compounds tested, **14b** showed a dose-response inhibition of PGE_2 production with an IC_{50} value of 2.1 μM. The suppression upon PGE_2 secretion was not due to cell death since **14b** did not reduce the cell viability in close proximity to the PGE_2 inhibition concentration. The obtained atomic coordinates for the single-crystal XRD of **14b** was then applied in the docking simulation to determine the potential important binding interactions with murine COX-2 and mPGES-1 putative binding sites.

Prostaglandin E_2 (PGE_2), a product of the cyclooxygenase (COX) pathway is well identified as the lipid mediator that contributes to inflammatory diseases such as cancer, rheumatoid arthritis, atherosclerosis, and pain.[1] The conversion of arachidonic acid into prostaglandin H_2 (PGH_2) is tightly regulated by cyclooxygenases and subsequently transformed to PGE_2 by either of the PGE synthases including microsomal prostaglandin E synthase-1 (mPGES-1), microsomal prostaglandin E synthase-2 (mPGES-2), and cytosolic prostaglandin E synthase (cPGES). Both cPGES and mPGES-2 are constitutively expressed in various organs/tissues, whilst mPGES-1, like COX-2, is up-regulated in response to various inflammatory stimuli (Fig. 1).[2–5]

Dihydrochalcones, prenylated chalcones, prenylated flavones, aurones, and prenylated aurones are categorised into the group of minor flavonoids.[6] These compounds have a unique and defined chemical structure, which are commonly found in the plant kingdom and possess many interesting biological activities. Additionally, the presence of prenyl group in the flavonoid ring system increases lipophilicity and bestows to the molecule a strong affinity for biological membranes. It also improves the pharmacokinetic profile of a compound leading to a broader range of interesting pharmacological activities.[7] As an example, xanthohumol (**1**), a prenylated chalcone, was found to be active in a wide range of anti-inflammatory activities.[8,9] Furthermore, a prenylated flavonoid namely sophoraflavanone G (**2**) inhibited prostaglandin E_2 (PGE_2) production from lipopolysaccharide (LPS)-treated RAW cells by down-regulating the COX-2 expression at 1–50 μM (IC_{50} = 2.7 μM).[10] Some of the aurones such as sulfuretin (**3**) derivatives have been synthesized and displayed remarkable inhibition results on PGE_2 production in LPS-induced RAW 264.7 cells to reveal the SAR of the compounds.[11] On the other hand, artocarpaurone (**4**), a newly isolated prenylated aurone from the methanol extract of *Artocarpus altilis* was found to exhibit NO radical scavenging activity (Fig. 2).[12]

* Corresponding author. Tel.: +60 3 9289 7031.
E-mail address: david_lam_98@yahoo.com (L.K. Wai).

http://dx.doi.org/10.1016/j.bmcl.2014.06.061
0960-894X/

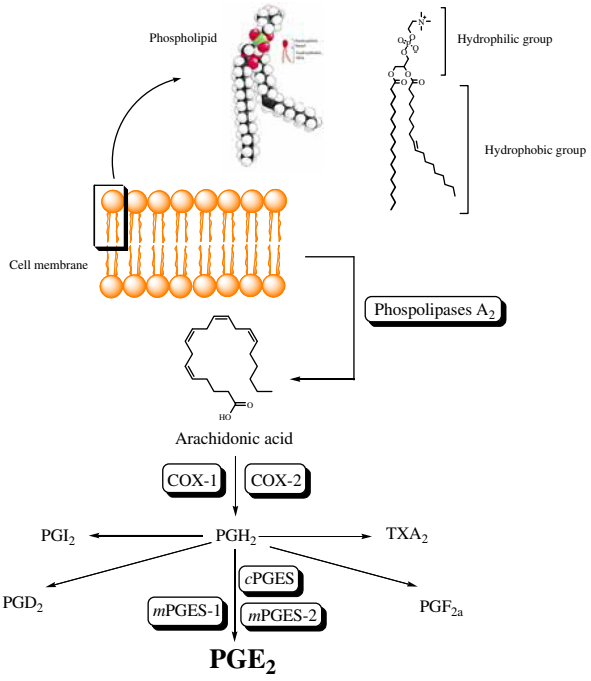

Figure 1. Biochemical conversion of PGE_2 from arachidonic acid.

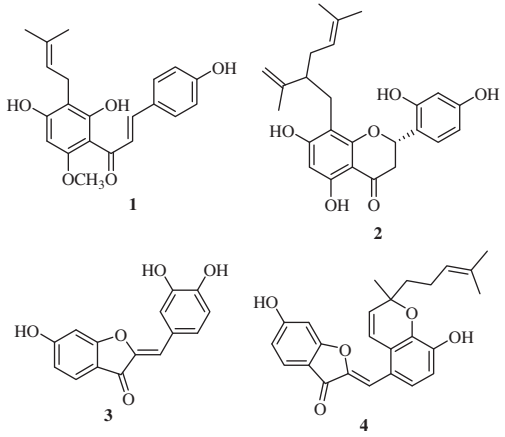

Figure 2. Selected minor flavonoids as potential anti-inflammatory agents.

In the present Letter, we have successfully synthesized 2′-hydroxychalcones, prenylated chalcones, flavonols, prenylated flavonols, aurones, and prenylated aurones. The preparation of the 2′-hydroxychalcone derivatives were carried out via the Claisen–Schmidt condensation (Scheme 1). Initially, 2′-hydroxy-4′-methoxy-acetophenone (**5**) was reacted with the commercially available appropriate aryl aldehyde derivatives (**6**) in the presence of KOH in EtOH to afford the corresponding crude 2′-hydroxychalcone derivatives. Subsequent neutralization with HCl yielded the desired products with average yields of 55–98%. The yield of the products could be further improved when the reaction was carried out under ultrasound irradiation at 40 °C.[13] On the other hand, the aryl aldehydes with hydroxyl substituent were first converted to the corresponding tetrahydropyranyl ethers to afford the final products with an improved overall percentage of yields (Scheme S1, Supplementary data). Next, the aurones were prepared via oxidative cyclisation method by reacting the 2′-hydroxychalcone derivatives (**7a**–**g**) with mercury (II) acetate in DMSO under reflux condition.[14] All products were purified using flash chromatography and recrystallised from EtOH to afford the corresponding aurones (**8a**–**c**) in low yields (22–27%). To produce the corresponding flavonols (**9a**–**c**), the 2′-hydroxychalcone derivatives were cyclised via a modified Algar–Flynn–Oyamada (AFO) reaction, using an aqueous hydrogen peroxide (30%) and NaOH (40%) in EtOH.[15,16] The conversion of the 2′-hydroxychalcone derivatives to the flavonols were successful using the conventional AFO reaction although the yields varied depending on the type of substituents in the aryl aldehydes used after flash chromatography and recrystallisation from EtOH. AFO reaction is a convenient method used in the synthesis of dihydroflavonols, aurones, and other flavonoid compounds.[17] In spite of this, we did not manage to isolate **9c** derived from chalcone bearing electron withdrawing dichloro groups; the product yield was not determined.

Several strategies were employed to introduce the prenyl group into the corresponding chalcones, flavonols, and aurones in this Letter. Addition of the prenyl group to the 3-hydroxyflavones was achieved by treating **9a**–**b** with 1-chloro-3-methyl-2-butene in the presence of K_2CO_3 in acetone under reflux condition. The desired products, **10a**–**b** were obtained in moderate to high yields (62–80%). Insertion of the geranyl group to the 3-position of the 3-hydroxyflavones successfully produced compounds **10c**–**d** in moderate yields (42–62%). Attempt to prenylate the ring system of **5** by direct alkylation using KOH,[18] however failed to yield any product. To facilitate the migration, a [3,3]-sigmatropic rearrangement approach was then adopted by refluxing compound **11** in *N*,*N*-dimethylaniline at 200 °C under nitrogen atmosphere to give the desired product in moderate yield. Based on the NMR result[19a] (Supplementary data), the prenyl group effectively migrated to the *para* position to give the *C*-prenylated product, **12** with 36% of yield after flash chromatography (Scheme 2). Replacing 3,3-dimethylallyl bromide with 1-chloro-3-methyl-2-butene, however, resulted in a low yield of **12**. It is important to mention that **11** was used directly in the subsequent reaction after the removal of K_2CO_3 by filtration which could resulted in the presence of 3,3-dimethylallyl bromide or 1-chloro-3-methyl-2-butene residue in the reaction mixture. It is possible that 3,3-dimethylallyl bromide residue might participate in the [3,3]-sigmatropic rearrangement reaction to form **12** based on our observation. On the other hand, we failed to introduce the prenyl group to the *ortho* position of compound **5** ring system by [1,3]-sigmatropic rearrangement by using montmorillonite K_{10} as a catalyst in CH_2Cl_2 at 0 °C, even-though a similar method was reported previously by Sugamoto et al.[20]

The Claisen–Schmidt condensation between **12** and aryl aldehyde derivatives (**6**) was performed in the presence of KOH base in EtOH under ultrasound irradiation at 40 °C to give the corresponding *C*-prenylated chalcones, (**14a**–**e**) in the range of low to high yields (12–80%). It is interesting to note that the cyclisation of **14a**–**b** in the presence of $Hg(OAc)_2$ in DMSO gave the desired *C*-prenylated aurones in moderate yields (33–44%) without affecting the stability of the prenyl group (Scheme 3). Only a few literatures have reported the synthesis of *C*-prenylated aurones up to date.[21,22] An alternative method is proposed here for the synthesis of *C*-prenylated aurones. On the other hand, two new *O*-prenylated aurone derivatives, **17a**–**b** were obtained in reasonable yields as shown in Scheme 4. Besides, we did not manage to isolate **22a**–**b**, the *C*-prenylated flavonols derivatives via the AFO reaction (Scheme S2, Supplementary data).

Preliminary screening results on PGE_2 production in LPS-induced RAW 264.7 cells showed that compounds **14a**–**e** demonstrated good PGE_2 inhibitory activity have prompted us to introduce bulky phenyl group to both R_1 and R_2 as shown in Scheme 5. A Suzuki coupling reaction was adopted utilising a simple formation of carbon-carbon single bond to give the new prenylated chalcone derivatives, **21a**–**b**.[23] The reactants (**20a**–**b**) were

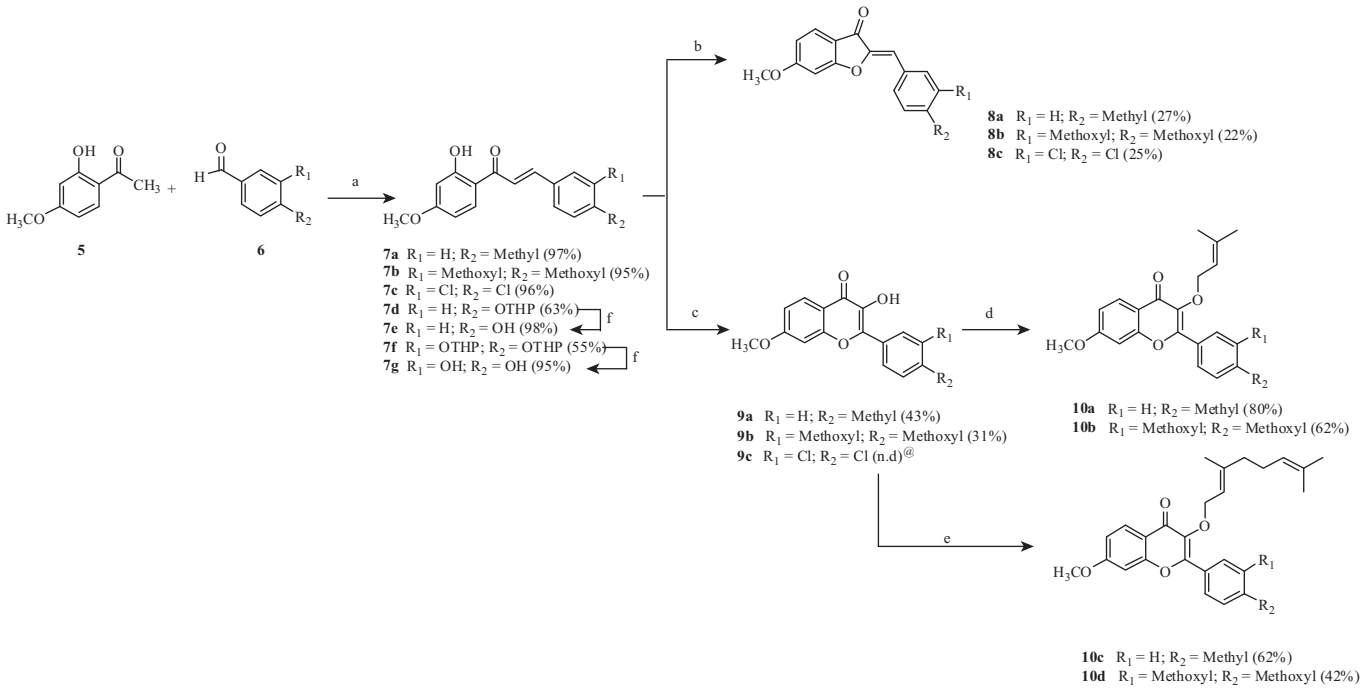

Scheme 1. Reagents and conditions of synthesis: (a) KOH 40%, EtOH, (i) sonicate 1 h at 40 °C (ii) stir at rt overnight; (b) $Hg(OAc)_2$, DMSO, reflux 160 °C, 6 h; (c) KOH 40%, H_2O_2, EtOH, rt 3–4 h; (d) 1-Chloro-3-methyl-2-butene, K_2CO_3, Acetone, reflux 75 °C, 20–24 h; (e) Geranyl bromide, K_2CO_3, Acetone, reflux 75 °C, 20–24 h (f) TsOH, MeOH, stir at rt 2 h. @Not determined due to purification problem.

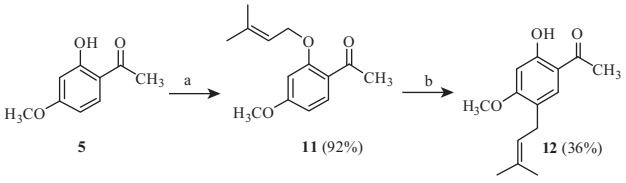

Scheme 2. Reagents and conditions of synthesis: (a) 3,3-dimethylallyl bromide, K_2CO_3, acetone, reflux 75 °C, 20 h; (b) DMA, reflux 200 °C under N_2 atmosphere.

obtained in reasonable yields (70% and 79%, respectively) according to the modified method using the Suzuki coupling reaction catalysed by in situ generated palladium nanoparticles in PEG-400 solvent under aerobic condition (Scheme 5). This oxygen-promoted ligand-free Suzuki coupling reaction was previously reported by Han et al.. The reaction is highly efficient for coupling aryl chlorides with phenylboronic acid in a short time under mild condition.[24] The Claisen–Schmidt condensation between **20a–b** and **12** yielded the desired products **21a–b** in moderate yields (34% and 48%, respectively) (Scheme 6).

The PGE_2 inhibitory activity of the synthesized compounds was evaluated using the mouse macrophage (RAW 264.7) cell line, stimulated by lipopolysaccharide (LPS) at the concentration of 50 μM.[19b] The results summarised in Table 1, showed that most

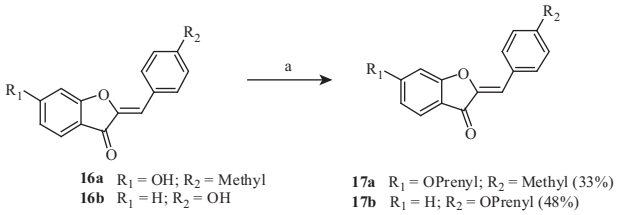

Scheme 4. Reagents and conditions of synthesis: (a) 1-Chloro-3-methyl-2-butene, K_2CO_3, acetone, reflux 75 °C, 20–24 h.

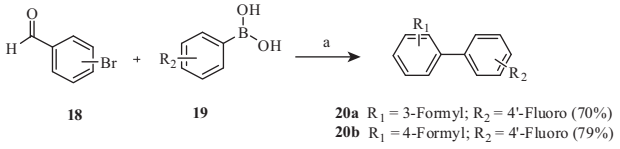

Scheme 5. Reagents and conditions of synthesis: (a) 4-fluorophenylboronic acid, $Pd(OAc)_2$, PEG 400, K_2CO_3, 60 °C 20 h.

of the synthesized compounds exhibited moderate to strong PGE_2 production inhibition (41–90%) except for compounds **7a**, **15a**, and **21b**, which displayed poor activity. Compound **7a** was

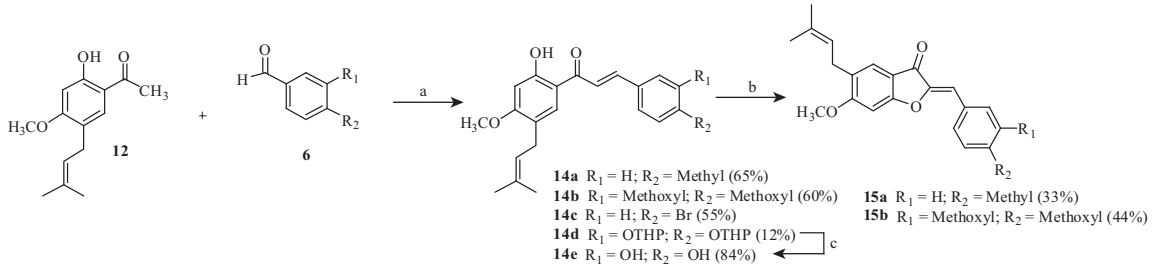

Scheme 3. Reagents and conditions of synthesis: (a) KOH 40%, EtOH, (i) sonicate 1 h at 40 °C (ii) stir at rt overnight; (b) $Hg(OAc)_2$, DMSO, reflux 160 °C, 6 h; (c) TsOH, MeOH, stir at rt 2 h.

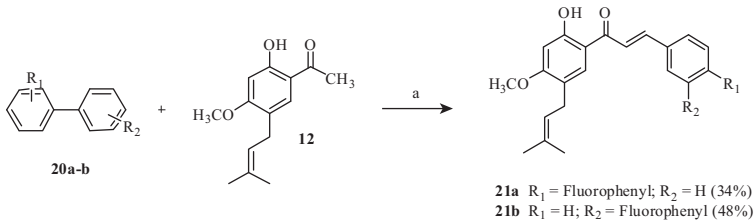

Scheme 6. Reagents and conditions of synthesis: (a) KOH 40%, EtOH, (i) sonicate 1 h at 40 °C (ii) stir at rt overnight.

Table 1
In vitro PGE_2 production inhibitory activities of synthesized compounds in LPS-induced RAW 267.4 cells

Compound	Percentage (%) inhibition of PGE_2 at 50 μM	$IC_{50}^{\pm}$ (μM)	Viability (%)
7a[*]	na		97
7b	75		>100
8a	78		>100
8b	76		>100
9a	70		78
9b	80		82
10a	41		62
10b	58		>100
14a	64		>100
14b[#]	90	2.1	>100
14c	70		>100
14e	61		>100
15a[*]	na		>100
15b	83		>100
17a	43		>100
17b	77		>100
21a	63		>100
21b[*]	na		>100
NS-398[∞]	97	0.1	>100

[*] na is not active.
[#] Most active compound.
[∞] NS-398 (*N*-(2-cyclohexyloxy)-4-nitromethanesulfonamide) was used as a reference compound.
[±] IC_{50} of the most active compound and the positive control, NS-398.

Table 2
Crystal and structure refinement parameters of compound **14b**

Identification code	
Empirical formula	$C_{23}H_{26}O_5$
Formula weight	382.44
Temperature	296(2) K
Wavelength	0.71073 Å
Crystal system, space group	Triclinic, P$\bar{1}$
Unit cell dimensions	a = 8.4547(13) Å
	b = 13.816(2) Å
	c = 18.621(3) Å
	α = 97.590(5)°
	β = 92.128(5)°
	γ = 105.061(5)°
Volume	2076.1(5) $Å^3$
Z, calculated density	4, 1.224 Mg/m3
Absorption coefficient	0.085 mm^{-1}
F(0 0 0)	816
Crystal size	0.330 × 0.260 × 0.150 mm^3
Theta range for data collection	3.087–24.998°
Limiting indices	$-10 \leqslant h \leqslant 10$, $-16 \leqslant k \leqslant 16$, $-22 \leqslant l \leqslant 21$
Reflections collected/unique	7281 [*R*(int) = 0.1322]
Completeness to theta = 25.00	96.9%
Refinement method	Full-matrix least-squares on F^2
Data/restraints/parameters	7281/3/514
Goodness-of-fit on F^2	1.119
Final R indices [I > 2sigma(I)]	*R*1 = 0.1308, wR_2 = 0.3994
R indices (all data)	*R*1 = 0.1763, wR_2 = 0.4348
Extinction coefficient	0.018(4)
Largest diff. peak and hole	0.508 and −0.363 e $Å^{-3}$

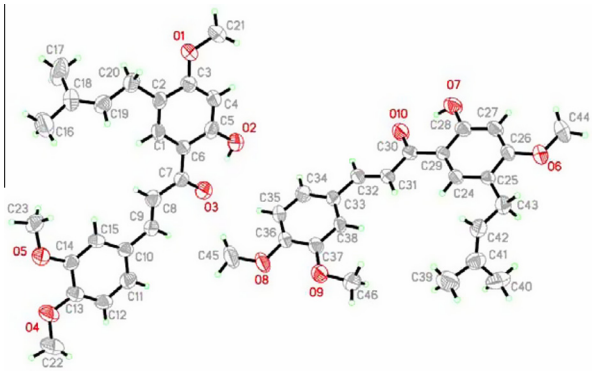

Figure 3. ORTEP diagram of the compound **14b** with thermal ellipsoids drawn at 50% probability.

inactive against PGE_2 production though **8a** (aurone) and **9a** (flavonol) which are the cyclised products of the α,β-unsaturated chalcone were found to be active. Insertion of the prenyl group to the 3-hydroxyflavone series was equally bad for the activity. On the other hand, compound **14b** (*E*)-3-(3,4-dimethoxyphenyl)-1-(4-methoxy-3-(3-methylbut-2-enyl)phenyl)-prop-2-en-1-one), the prenylated chalcone, significantly suppressed PGE_2 production with 90% of inhibition was found to be comparable to the result of the positive inhibitor, NS-398. Further test showed that **14b** suppressed the production of PGE_2 with an IC_{50} value of 2.1 μM. Based on the preliminary results, the prenylated chalcones (**14a**–**e**) were found to be highly potent against PGE_2 synthesis. Currently, we are synthesizing and optimising this series of compounds and a full SAR study will be reported in the near future. Nevertheless, it is critical to note that the position of fluorophenyl group of compounds **21a** and **21b** was also decisive for the inhibitory activity. Apparently, the presence of the fluorophenyl group at *para* position resulted in the moderate inhibition as displayed by **21a** while at *meta* position, compound **21b** did not demonstrate any inhibition. This remarkable observation will definitely serve as an important point in the future design of PGE_2 synthesis inhibitors using the template structure of **21a**. The cytotoxic effect of the synthetic compounds was also evaluated using the MTT assay to test whether the inhibitory effect on the production of PGE_2 was due to cell cytotoxicity. Most of the synthesized compounds were non-cytotoxic to RAW 264.7 cells at 50 μM concentration. Additionally, compound **14b** was tested for the NO inhibition and was found to exhibit an IC_{50} value of 13.8 μM. Figure 5 shows the dose–response of **14b** towards the secretion of PGE_2 and NO.

All ^1H NMR, ^{13}C NMR and ESI-HRMS spectra were consistent with the assigned structures of the synthesized compounds (Supplementary data).[19a] The characterisation of the most active compound **14b** was conducted by a single crystal X-ray structural analysis.[19c] It was difficult to obtain a good quality crystal but after several attempts of recrystallisation, sufficient reflections for structural solution with R*1* value of 13% was finally achieved. The compound crystallized

Table 3
Selected geometric parameter of compound **14b** (Å, °)

C1–C2	1.371(10)	O1–C3	1.351(6)
C2–C3	1.411(10)	O2–C5	1.341(10)
C3–C4	1.368(11)	O3–C7	1.269(10)
C4–C5	1.392(11)	O4–C13	1.361(10)
C5–C6	1.431(10)	O5–C14	1.353(10)
C1–C6	1.406(10)	C6–C7	1.446(10)
C18–C19	1.321(11)	C7–C8	1.473(11)
C41–C42	1.332(11)	C8–C9	1.327(11)
O3–C7	1.268(9)	C18–C19	1.319(12)
O2–C5	1.341(9)	O6–C26	1.356(10)
O1–C3	1.351(9)	O7–C28	1.329(10)
O5–C14	1.353(9)	O8–C36	1.375(9)
O4–C13	1.350(9)	O9–C37	1.354(9)
C10–C11	1.383(10)	O10–C30	1.258(9)
C11–C12	1.388(11)	C29–C30	1.457(10)
C12–C13	1.367(11)	C31–C32	1.318(10)
C13–C14	1.401(10)	C32–C33	1.466(10)
C14–C15	1.385(10)		
C10–C15	1.392(10)	C41–C42	1.333(11)
C13–O4–C22	117.5(7)	C8–C9–C10	126.8(7)
C14–O5–C23	118.0(6)	C29–C30–C31	120.2(6)
C3–O1–C21	118.3(7)	C30–C31–C32	122.9(7)
C6–C7–C8	120.5(6)		
C7–C8–C9	122.4(7)	C31–C32–C33	126.8(7)

in a triclinic system with space group Pī, $a = 8.4547(13)$ Å, $b = 13.816(2)$ Å, $c = 18.621(3)$ Å, $\alpha = 97.590(5)°$, $\beta = 92.128(5)°$, $\gamma = 105.061(5)°$, $Z = 4$ and $V = 2076.1(5)$ Å^3. The crystal system and refinement data are shown in Table 2. The asymmetric unit consists of two independent molecules (Fig. 3). The molecules are apparently planar. However, the dihedral angles between 1-(2-hydroxy-4-methoxy-5-(3-methylbut-2-enyl)phenyl)propanyl-1-one, O1/O2/O3/(C1-C9)/C20/C21 and 1,2-dimethoxy-4-methylbenzene, O4/O5/(C9-C15)/C22/C23 fragments in the first molecule, and O6/O7/O10/(C24-C32)/C43/C44 and O8/O9/(C32-C38)/C45/ C46 in the second molecule are 7.32(19)° and 6.61(18)°, respectively. All the fragments are planar with maximum deviation of 0.072(6) Å for O10 atom from the least square plane of the O6/O7/O10/(C24-C32)/C43/C44 fragment. Both molecules adopt *trans* configuration with

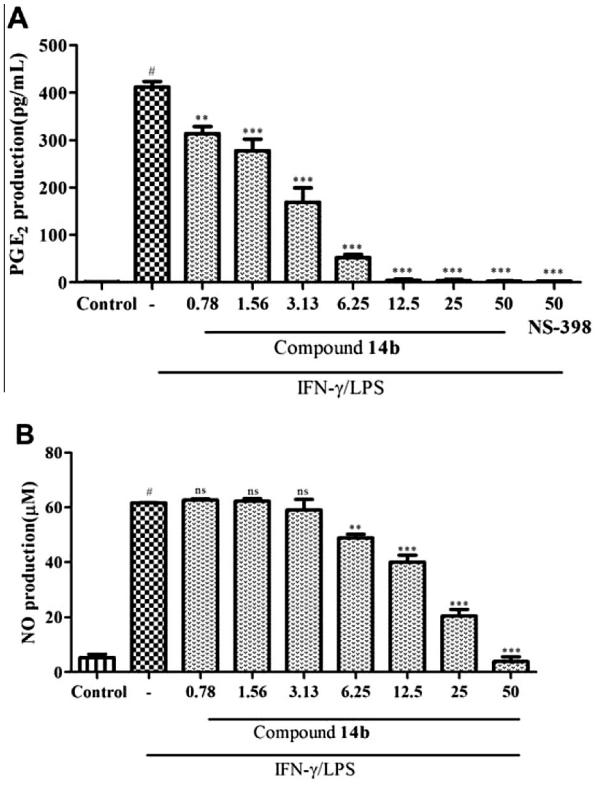

Figure 5. Effects of **14b** on (a) PGE_2 and (b) NO production in LPS-stimulated RAW 264.7 cells. The cells were co-incubated with LPS (5 μg/mL) and different concentrations of **14b** ranging from 0.78 to 50 μM. The supernatants were then collected for the measurement of PGE_2 and NO production using EIA kit and a Griess reagent, respectively. **14b** significantly inhibited PGE_2 and NO levels in LPS stimulated macrophages. The values are expressed as the means ± SD of three individual samples. $^{***}P < 0.001$ as compared with the LPS-treated macrophages; significant differences between groups were determined using one-way ANOVA test followed by a Dunnett's multiple comparison test. $^{\#}P < 0.05$ solvent control compared with the LPS-treated cells; significant difference was determined using unpaired student's *t*-test (ns is not significant).

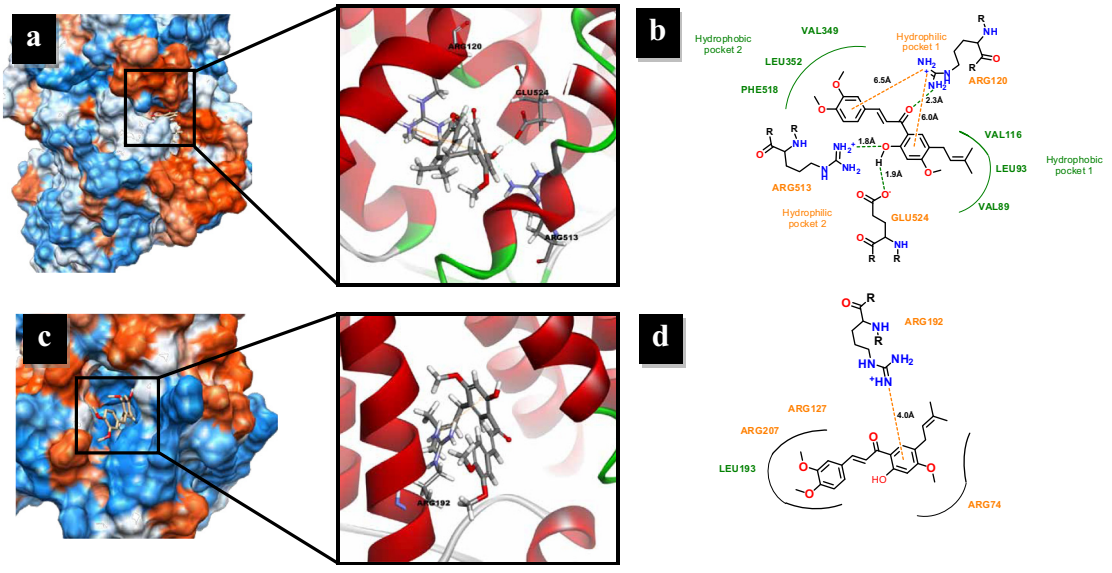

Figure 4. Predicted binding poses retrieved from flexible docking of **14b** in (a) the murine COX-2 and (b) murine mPGES-1 (homology model) putative binding sites. The atom colouring for the compounds is the following: carbons in grey, oxygen in red, nitrogen in blue, and hydrogen in white. (b) and (d) represent the 2D diagram of binding interactions between **14b** with the active site of murine COX-2 and murine mPGES-1(homology model), respectively. Hydrogen atoms have been omitted in the 2D diagram for clarity. The orange line indicates the π-interaction, while the green line indicate the hydrogen-bonding interactions, with distance indicated in angstroms, Å.

respect to the position of the 1-(2-hydroxy-4-methoxy-5-(3-methylbut-2-enyl)phenyl)-propanyl-1-one and 1,2-dimethoxy-4-benzene groups across their C8-C9 and C31-C32 double bonds of 1.321(10) and 1.318(10) Å, respectively. Other bond lengths and angles are in normal ranges as shown in Table 3. There are O2-H2A...O3 and O7-H7A...O10 intramolecular hydrogen bonds in the molecules. The structure is stabilised by C23-H23A...O4 ($1-x$, $2-y$, $-z$; D...A = 3.469(12) Å and D...H...A = 165°) and C46-H46A...O8 ($1-x$, $1-y$, $1-z$; D-H= 3.427(11) Å and D-H...A = 162°) intermolecular hydrogen bonds. The crystallographic data for the structural analysis were deposited with the Cambridge Crystallographic Data Centre No **997318**.

To elucidate the possible binding interactions of compound **14b**, the protein crystal structures of murine COX-2 (**6COX**: 2.8 Å) and human mPGES-1 (**4AL0**: 1.2 Å) were retrieved from Brookhaven Protein Data Bank. The obtained single crystal-XRD atomic coordinates for **14b** was then employed in the docking study (see Fig. 3). Since the complete crystallised three-dimensional structure of murine mPGES-1 is currently not available, we attempted to build a homology model from the human protein crystal structure mPGES-1 (**4AL0**: 1.2 Å).[25] We selected the non-conserved region in human mPGES-1 as the putative binding site for compound **14b** based on the fact that MK-886 inhibitor selectively inhibit human mPGES-1 activity while weakly against murine mPGES-1. The murine mPGES-1 homology model built was used as a molecular target in the docking experiment. Further analysis on the sequence alignment revealed that human and murine mPGES-1 share 77.1% of their sequence identity and have 84.3% of sequence similarity, which supports the use of **4AL0** as a suitable template for building the murine homology model, and these proteins potentially share a conserved common folding (Fig. S1, Supplementary Data). The quality of the refined homology model was then assessed by Ramachandran plots and PROCHECK analyses, which revealed that most of the residues were in favored regions: 93.7% most favored, 5.3% additional allowed, 0.3% generously allowed, and 0.8% disallowed. All the critical points were located away from the putative binding site (Figs. S2 & S3 and Table S1, Supplementary Data).

In order to check the CHARMm flexible docking efficiency in reproducing the X-ray structure, the co-crystallised ligand of the pdb file (**6COX**) was extracted and redocked using the default settings (Fig. S4, Supplementary Data). The RMSD between the top ranked pose and the crystal structure was found consistent (RMSD value 0.65 Å). According to the docking results, compound **14b** participates in a number of important binding interactions in the active site of murine COX-2 than murine mPGES-1 (homology model) (Fig. 4). Near the surface active site of murine COX-2, compound **14b** interacts with the side chains of Arg120, Arg513, and Glu524. The docking results showed that both the aromatic rings of **14b** form weak cation-π interaction with the protonated amino-side chain of residue Arg120, which is located in the hydrophilic pocket 1 by about 6.5 Å and 6.0 Å (aromatic ring—$^{+}H_2N$–), respectively. In the hydrophilic pocket 2, the hydroxyl group of **14b** engaged with Arg513 and Glu524 residues through H-bonding molecular interaction within distances of 1.8 Å and 1.9 Å (HO—$^{+}H_2$-N– and HO—$^{-}$OOC–), respectively. Such interactions are almost essential for the COX-2 inhibitory activity based on the binding interactions displayed by the ligand co-crystal of SC-558, an analogue of celecoxib, in the COX-2 active site.[26,27] Nonetheless, residue Arg513 has been identified as the key contributor to COX-2 specificity while in COX-1, this residue is replaced by a histidine residue. The presence of Arg513 residue results in a stable positive charge group being placed at the center of the pocket.[28] It is also known that, this residue is a crucial requirement for the time-dependent inhibition of COX-2. This arginine residue appears to

Table 4
ADMET profile prediction of the synthesized compounds

Compd	ADMET parameter									
	Human Intestinal Absorption			Aqueous Solubility		Blood Brain Barrier (BBB) Penetration		Plasma Protein Binding (PPB)	Cytochrome P_{450} 2D6 (CYP2D6)	Hepatotoxicity
	PSA[a]	AlogP98[b]	Level[c]	Log (*Sw*)[d]	Level[e]	LogBB[f]	Level[g]	Prediction[h]	Prediction[i]	Prediction[j]
7a	47.046	3.929	0	−4.195	2	0.316	1	1	0	1
7b	64.906	3.410	0	−3.821	3	−0.127	2	1	0	1
8a	35.160	3.606	0	−4.829	2	0.404	1	1	0	1
8b	53.021	3.087	0	−4.301	2	−0.039	2	1	0	1
9a	55.976	3.068	0	−4.031	2	−0.091	2	1	0	1
9b	73.836	2.549	0	−3.664	3	−0.534	3	1	0	1
10a	44.091	4.759	0	−5.789	2	0.619	1	1	0	1
10b	61.951	4.240	0	−5.188	2	0.176	1	1	0	0
14a	47.046	5.786	0	−5.781	2	0.890	0	1	0	1
14b[#]	64.906	5.267	0	−5.313	2	0.447	1	1	0	1
14c	47.046	6.048	1	−6.095	1	0.971	0	1	0	1
14e	88.677	4.816	0	−4.503	2	—	4	1	0	1
15a	35.160	5.462	0	−6.433	1	0.978	0	1	0	1
15b	53.021	4.943	0	−5.811	2	0.535	1	1	0	1
17a	35.160	5.071	0	−5.989	2	0.857	0	1	0	0
17b	35.160	4.585	0	−5.490	2	0.707	0	1	0	0
21a	47.046	7.024	3	−6.855	1	—	4	1	0	1
21b	47.046	7.024	3	−6.915	1	—	4	1	0	1

[#] Most active compound.
[a] Polar surface area (PSA) (>150: very low absorption).
[b] Atom-based logP (AlogP98) ($\leqslant -2.0$ or $\geqslant 7.0$: very low absorption).
[c] Level of human intestinal absorption prediction; 0 (good), 1 (moderate), 2 (poor), 3 (very poor).
[d] The based ^{10}logarithm of the molar solubility log(*Sw*) (25 °C, pH = 7.0) (acceptable drug-like compounds: $-6 < \log(Sw) \leqslant 0$).
[e] Level of aqueous solubility prediction; 0 (extremely low), 1 (very low), 2 (low), 3 (good), 4 (optimal), 5 (too soluble), 6 (warning: molecules with one or more unknown AlogP calculation).
[f] Very high penetrants (logBB $\geqslant$ 0.7).
[g] Level blood brain barrier penetration prediction; 0 (very high penetrate), 1 (high), 2 (medium), 3 (low), 4 (undefined).
[h] Prediction Plasma-protein binding (0: <90%; 1: $\geqslant$90%;).
[i] Prediction cytochrome P_{450} 2D6 enzyme inhibition (0: non-inhibitor; 1: inhibitor).
[j] Prediction hepatotoxicity (0: non-toxic; 1: toxic).

interact with the hydroxyl substituent of **14b**. On the other hand, the prenyl substituent of **14b** is well-positioned in the hydrophobic pocket 1, constituting of hydrophobic residues Val116, Leu93, and Val89 in the COX-2 active site. The presence of this group could possibly increase the ligand binding affinity and thus resulted in higher inhibitory activity of **14b**. However, **14b** were predicted to bind poorly to the murine mPGES-1 active site. The docking result in Figure 4, showed that the aromatic ring of **14b** could only form a weak cation-π interaction with the protonated amino-side chain of residue Arg192 of about 4.0 Å (aromatic-ring—$^{+}H_2N$–).

Pharmacokinetic is the study of what happens to drugs as they are administered and pass through the body. Poor clinical safety and toxicity contributes significantly to clinical failures in drug discovery. The ADMET profile of the synthesized compounds was assessed by the standard descriptors protocol implemented in Discovery Studio® 3.1. The parameters included in the analysis were human intestinal absorption (HIA), aqueous solubility, blood brain barrier (BBB) penetration, cytochrome P450 2D6 (CYP2D6) enzyme inhibition, hepatotoxicity, plasma-protein binding (PPB), atom-based logP (AlogP98), and polar surface area (PSA). According to the values presented in Table 4, all of the compounds except **21a** and **21b**, can be efficiently absorbed in the human intestine. The most potent compound, **14b** also showed promising logarithm of the molar solubility value of −5.313 for the aqueous solubility. On a positive note, **14b** does not exhibit very high BBB penetration and it does not inhibit the cytochrome P_{450}, which means that the compound can readily undergo oxidation and hydroxylation in the first phase of metabolism. Although the in silico prediction reveals that **14b** is hepatotoxic, further structural modifications can be done to improve the toxicity profile of the compound.

In conclusion, a series of novel minor chalcone and flavonoid compounds have been synthesized and their effects on PGE_2 production in LPS-induced RAW 264.7 cells were evaluated. Prenylated chalcone (**14b**) exhibited the highest inhibition on PGE_2 production with an IC_{50} value of 2.1 μM and was non-cytotoxic at the tested concentration. Docking study revealed that **14b** could bind favorably to COX-2 and will serve as an important template for future chemical modification. Future studies will address on the SAR study of **14b** as a potential PGE_2 synthesis inhibitor.

Acknowledgments

This work was financially supported by Science Fund (02-01-02-SF00665), Ministry of Science, Technology & Innovation, Malaysia. Authors also thank University Kebangsaan Malaysia for the funds provided under the Research University Grant (GUP) (UKM-GUP02011-014) and UKM-DIP-2012-11. We thank Prof. Dr. Simon Gibbons and Mr. Mohd Syukri Baharuddin for valuable comments on different parts of the manuscript.

A. Supplementary data

Supplementary data associated with this article can be found, in the online version, at http://dx.doi.org/10.1016/j.bmcl.2014.06.061. These data include MOL files and InChiKeys of the most important compounds described in this article.

References and notes

1. Kawabata, A. *Biol. Pharm. Bull.* **2011**, *34*, 1170.
2. Legler, D. F.; Bruckner, M.; Uetz-von Allmen, E.; Krause, P. *Int. J. Biochem. Cell Biol.* **2010**, *42*, 198.
3. Funk, C. D. *Science* **1871**, *2001*, 294.
4. Fahmi, H. *Curr. Opin. Rheumatol.* **2004**, *16*, 623.
5. Jegerschöld, C.; Pawelzik, S.-C.; Purhonen, P.; Bhakat, P.; Gheorghe, K. R.; Gyobu, N.; Mitsuoka, K.; Morgenstern, R.; Jakobsson, P.-J.; Hebert, H. *Proc. Natl. Acad. Sci.* **2008**, *105*, 11110.
6. Ninomiya, M.; Koketsu, M. In *Natural Products*; Ramawat, K. G., Mérillon, J.-M., Eds.; Springer: Berlin, Heidelberg, 2013; p 1867.
7. Botta, B.; Vitali, A.; Menendez, P.; Misiti, D.; Monache, G. D. *Curr. Med. Chem.* **2005**, *12*, 713.
8. Lee, I.-S.; Lim, J.; Gal, J.; Kang, J. C.; Kim, H. J.; Kang, B. Y.; Choi, H. J. *Neurochem. Int.* **2011**, *58*, 153.
9. Cho, Y.-C.; Kim, H. J.; Kim, Y.-J.; Lee, K. Y.; Choi, H. J.; Lee, I.-S.; Kang, B. Y. *Int. Immunopharmacol.* **2008**, *8*, 567.
10. Kim, D.; Chi, Y.; Son, K.; Chang, H.; Kim, J.; Kang, S.; Kim, H. *Arch. Pharmacal Res.* **2002**, *25*, 329.
11. Shin, S. Y.; Shin, M. C.; Shin, J.-S.; Lee, K.-T.; Lee, Y. S. *Bioorg. Med. Chem. Lett.* **2011**, *21*, 4520.
12. Huong, T. T.; Cuong, N. X.; Tram, L. H.; Quang, T. T.; Duong, L. V.; Nam, N. H.; Dat, N. T.; Huong, P. T. T.; Diep, C. N.; Kiem, P. V.; Minh, C. V. *J. Asian Nat. Prod. Res.* **2012**, *14*, 923.
13. Li, J.-T.; Yang, W.-Z.; Wang, S.-X.; Li, S.-H.; Li, T.-S. *Ultrason. Sonochem.* **2002**, *9*, 237.
14. Narsinghani, T.; Sharma, M.; Bhargav, S. *Med. Chem. Res.* **2013**, *22*, 4059.
15. Li, Z.; Ngojeh, G.; DeWitt, P.; Zheng, Z.; Chen, M.; Lainhart, B.; Li, V.; Felpo, P. *Tetrahedron Lett.* **2008**, *49*, 7243.
16. Pandurangan, N.; Bose, C.; Banerji, A. *Bioorg. Med. Chem. Lett.* **2011**, *21*, 5328.
17. Bennett, M.; Burke, A. J.; Ivo O'Sullivan, W. *Tetrahedron* **1996**, *52*, 7163.
18. Diller, R. A.; Riepl, H. M.; Rose, O.; Frias, C.; Henze, G.; Prokop, A. *Chem. Biodivers.* **2005**, *2*, 1331.
19. *(a) Representative synthetic procedures and spectral characterizations.* Procedure for preparation of **1-(4-methoxy-2-(3-methylbut-2-enyloxy)-phenyl)ethanone (11)**. A mixture of **5** (3 g, 18.05 mmol), anhydrous K_2CO_3 (9.98 g, 72.20 mmol), and 3,3-dimethylallyl bromide (5.38 g, 36.10 mmol) was stirred in acetone (30 mL) and heated at 75 °C for 20 h. The reaction mixture was monitored by TLC. After completion of the reaction, the reaction mixture was filtrated and evaporated under vacuum. The residue was purified by silica gel flash column chromatography with *n*-hexane/EtOAc (gradient 0–30% EtOAc) to afford compound **11** (3.89 g, 92%) as colorless oil; R_f (10% EtOAc/*n*-hexane) 0.325; ^{1}H NMR (500 MHz, $CDCl_3$) δ 7.85 (d, *J* = 8.7 Hz, 1H), 6.53 (dd, *J* = 8.7, 2.3 Hz, 1H), 6.47 (d, *J* = 2.2 Hz, 1H), 5.53 (t, 1H), 4.61 (d, *J* = 6.6 Hz, 2H), 3.87 (s, 3H), 2.60 (s, 3H), 1.82 (s, 3H), 1.78 (s, 3H). ^{13}C NMR (126 MHz, CDCl3) δ 198.04, 164.38, 160.44, 138.34, 132.62, 119.06, 105.08, 100.86, 99.33, 65.42, 55.49, 32.01, 25.72, 18.26.
Procedure for preparation of **1-(2-hydroxy-4-methoxy-5-(3-methylbut-2-enyl)phenyl)ethanone (12)**. Intermediate **11** (3 g, 12.8 mmol) was dissolved in 10 mL of dimethylaniline and heated at 200 °C for 4 h. Ethyl acetate (50 mL) was added and the mixture was washed with 10% aq HCl (3 × 50 mL). The organic layer was dried over magnesium sulfate anhydrous, filtered, and evaporated. The residue was purified by silica gel flash column chromatography with *n*-hexane/EtOAc (gradient 0–50% EtOAc) to afford compound **12** (3.89 g, 36%) as colorless yellow oil; R_f (10% EtOAc/*n*-hexane) 0.45; ^{1}H NMR (500 MHz, $CDCl_3$) δ 12.72 (s, 1H), 7.42 (s, 1H), 6.41 (s, 1H), 5.28 (t, 1H), 3.88 (s, 3H), 3.24 (d, *J* = 7.2 Hz, 2H), 2.56 (s, 3H), 1.78 (s, 3H), 1.73 (s, 3H). ^{13}C NMR (126 MHz, $CDCl_3$) δ 202.52, 164.07, 163.89, 133.05, 130.73, 122.03, 121.68, 113.18, 99.05, 55.68, 27.77, 26.17, 25.76, 17.76. ESI-HRMS: ($C_{14}H_{18}O_3$) calc. [M+H] 235.1335, found 235.1320.
General procedure for preparation of 2′-hydroxychalcone derivatives. aq KOH (40%, 15 mL) was added to a stirred solution of acetophenone derivates (10 mmol) and (10 mmol) in absolute EtOH (30 mL). The mixture was sonicated for 1 h and was then stirred at room temperature overnight. The dark red solution was acidified with 2 M aq HCl to form a yellow precipitate, which was filtered and rinsed with distilled water. The precipitate was purified by flash chromatography with *n*-hexane/EtOAc (gradient 10–60% EtOAc) and recrystallisation using absolute EtOH. **(*E*)-1-(2-hydroxy-4-methoxyphenyl)-3-*p*-tolylprop-2-en-1-one (7a)**. Yellow solid, yield 97%, mp 120–121 °C; ^{1}H NMR (500 MHz, $CDCl_3$) δ 13.50 (s, 1H), 7.90 (d, *J* = 15.4 Hz, 1H), 7.86 (d, *J* = 8.6 Hz, 1H), 7.57 (dd, *J* = 15.5, 8.0 Hz, 3H), 7.26 (d, *J* = 7.9 Hz, 2H), 6.53–6.49 (m, 2H), 3.88 (s, 3H), 2.43 (s, 3H). ^{13}C NMR (126 MHz, $CDCl_3$) δ 191.97, 166.69, 166.17, 144.51, 141.25, 132.11, 131.21, 129.75, 128.58, 119.31, 114.18, 107.67, 101.11, 55.58, 21.53. ESI-HRMS: ($C_{17}H_{16}O_3$) calc. [M+Na$^+$] 291.0997, found 291.0984. **(*E*)-3-(3,4-dimethoxyphenyl)-1-(2-hydroxy-4-methoxy-phenyl)prop-2-en-1-one (7b)**. Yellow solid, yield 95%, mp 157–159 °C; ^{1}H NMR (500 MHz, $CDCl_3$) δ 13.56 (s, 1H), 7.88 (d, *J* = 7.4 Hz, 1H), 7.85 (s, 1H), 7.46 (d, *J* = 15.4 Hz, 1H), 7.27 (dd, *J* = 8.3, 1.8 Hz, 1H), 7.18 (d, *J* = 1.9 Hz, 1H), 6.93 (d, *J* = 8.3 Hz, 1H), 6.51 (dd, *J* = 11.5, 2.5 Hz, 2H), 3.99 (s, 3H), 3.96 (s, 3H), 3.88 (s, 3H). ^{13}C NMR (126 MHz, $CDCl_3$) δ 191.95, 166.81, 166.24, 151.79, 149.50, 144.72, 131.26, 127.99, 123.44, 118.23, 114.31, 111.38, 110.51, 107.78, 101.23, 56.17, 55.71. ESI-HRMS: ($C_{18}H_{18}O_5$) calc. [M+Na$^+$] 337.1052, found 337.1078. **(*E*)-1-(2-hydroxy-4-methoxy-5-(3-methylbut-2-enyl)phenyl)-3-*p*-tolyl prop-2-en-1-one (14a)**. Needle-yellow crystals, yield 65%, mp 119–120 °C; ^{1}H NMR (500 MHz, $CDCl_3$) δ 13.46 (s, 1H), 7.88 (d, *J* = 15.5 Hz, 1H), 7.62 (s, 1H), 7.56 (t, 3H), 7.27 (d, *J* = 8.0 Hz, 2H), 6.47 (s, 1H), 5.31 (t, 1H), 3.90 (s, 3H), 3.29 (d, *J* = 7.1 Hz, 2H), 2.43 (s, 3H), 1.80 (s, 3H), 1.76 (s, 3H). ^{13}C NMR (126 MHz, $CDCl_3$) δ 192.05, 165.54, 164.36, 144.24, 141.27, 133.14, 132.41, 129.90, 128.66, 122.43, 121.79, 119.76, 113.58, 99.53, 55.86, 28.15, 25.91, 21.69, 18.00. ESI-HRMS: ($C_{22}H_{24}O_3$) calc. [M+H] 337.1804, found 337.1811. **(*E*)-3-(3,4-dimethoxyphenyl)-1-(2-hydroxy-4-methoxy-5-(3-methylbut-2-enyl) phenyl)prop-2-en-1-one (14b)**. Needle-yellow crystals, yield 60%, mp 132–133 °C; ^{1}H NMR (500 MHz, $CDCl_3$) δ 13.51 (s, 1H), 7.85 (d, *J* = 15.4 Hz, 1H), 7.62 (s, 1H), 7.45 (d, *J* = 15.4 Hz, 1H), 7.27 (d, *J* = 8.4 Hz, 1H), 7.19 (s, 1H), 6.94 (d, *J* = 8.3 Hz, 1H), 6.47 (s, 1H), 5.32 (t, 1H), 3.99 (s, 3H), 3.97 (s, 3H), 3.90 (s, 3H), 3.29 (d, *J* = 7.1 Hz, 2H), 1.80 (s, 3H), 1.76 (s, 3H). ^{13}C NMR (126 MHz, $CDCl_3$) δ 191.83, 165.51, 164.26, 151.68, 149.47, 144.23, 133.18, 129.71, 128.12, 123.35, 122.41, 121.62, 118.52, 113.54, 111.39, 110.38, 99.51, 56.17, 56.08, 55.85, 27.99, 25.90,

17.98. ESI-HRMS: ($C_{23}H_{26}O_5$) calc. [M+H] 383.1859, found 383.1856. **(*E*)-3-(4-bromophenyl)-1-(2-hydroxy-4-methoxy-5-(3-methylbut-2-enyl) phenyl)-prop-2-en-1-one (14c)**. Needle-yellow crystals, yield 55%, mp 138–140 °C; ^{1}H NMR (500 MHz, CDCl^3) δ 13.35 (s, 1H), 7.81 (d, *J* = 15.5 Hz, 1H), 7.60 (s, 1H), 7.59 (d, *J* = 2.7 Hz, 2H), 7.57 (d, *J* = 15.7 Hz, 1H), 7.53 (d, *J* = 8.5 Hz, 2H), 6.47 (s, 1H), 5.30 (t, 1H), 3.91 (s, 3H), 3.28 (d, *J* = 7.1 Hz, 2H), 1.80 (s, 3H), 1.76 (s, 3H). ^{13}C NMR (126 MHz, $CDCl_3$) δ 191.59, 165.68, 164.60, 142.68, 134.06, 133.20, 132.41, 131.82, 129.94, 129.84, 124.95, 122.35, 122.01, 121.41, 113.47, 100.15, 99.57, 55.90, 28.17, 25.92, 18.01. ESI-HRMS: ($C_{21}H_{21}BrO_3$) calc. [M+H] 401.0753, found 401.0735. **(*E*)-3-(3,4-dihydroxyphenyl)-1-(2-hydroxy-4-methoxy-5-(3-methylbut-2-enyl)phenyl)prop-2-en-1-one (14e)**. Brown solid, 10%, mp 166–168 °C; ^{1}H NMR (500 MHz, MeOD) δ 7.71 (t, 2H), 7.48 (d, *J* = 15.3 Hz, 1H), 7.17 (d, *J* = 2.0 Hz, 1H), 7.10 (dd, *J* = 8.2, 1.9 Hz, 1H), 6.83 (d, *J* = 8.2 Hz, 1H), 6.46 (s, 1H), 5.29 (t, *J* = 7.3, 5.9, 1.4 Hz, 1H), 3.87 (s, 3H), 3.27 (d, *J* = 7.2 Hz, 2H), 1.76 (s, 3H), 1.74 (s, 3H). ^{13}C NMR (126 MHz, MeOD) δ 192.22, 164.85, 164.16, 148.60, 145.50, 144.77, 132.06, 129.73, 127.01, 122.33, 122.13, 121.59, 116.93, 115.24, 114.44, 113.13, 98.70, 54.85, 27.60, 24.50, 16.47. ESI-HRMS: ($C_{21}H_{22}O_5$) calc. [M+H] 355.1546, found 355.1534. **(*E*)-3-(4'-Fluoro-4-biphenylyl)-1-(2-hydroxy-4-methoxy-phenyl)-2-propen-1-one (21a)**. Yellow solid, yield 34%, mp 150–151 °C; ^{1}H NMR (500 MHz, $CDCl_3$) δ 13.44 (s, 1H), 7.93 (d, *J* = 15.5 Hz, 1H), 7.74 (d, *J* = 8.2 Hz, 2H), 7.66–7.61 (m, 6H), 7.20–7.16 (m, 2H), 6.48 (s, 1H), 5.32 (t, 1H), 3.91 (s, 3H), 3.30 (d, *J* = 7.2 Hz, 2H), 1.81 (s, 3H), 1.77 (s, 3H). ^{13}C NMR (126 MHz, $CDCl_3$) δ 191.82, 165.65, 164.50, 143.53, 142.36, 136.43, 134.11, 133.18, 130.89, 129.89, 129.19, 128.87, 128.81, 127.64, 122.41, 121.92, 120.75, 116.11, 115.94, 113.58, 99.57, 68.00, 55.89, 28.17, 25.93, 18.02. ESI-HRMS: ($C_{27}H_{25}FO_3$) calc. [M+H] 417.1867, found 417.1856. **(*E*)-3-(4'-Fluoro-3-biphenylyl)-1-(2-hydroxy-4-methoxy-phenyl)-2-propen-1-one (21b)**. Yellow crystals, yield 48%, mp 125–126 °C; ^{1}H NMR (500 MHz, $CDCl_3$) δ 13.41 (s, 1H), 7.95 (d, *J* = 15.5 Hz, 1H), 7.82 (s, 1H), 7.68–7.59 (m, 6H), 7.53 (t, *J* = 7.7 Hz, 1H), 7.19 (t, *J* = 8.6 Hz, 2H), 6.48 (s, 1H), 5.32 (t, 1H), 3.91 (s, 3H), 3.29 (d, *J* = 7.2 Hz, 2H), 1.81 (s, 3H), 1.76 (s, 3H). ^{13}C NMR (126 MHz, $CDCl_3$) δ 191.79, 165.67, 164.55, 161.93, 143.83, 141.30, 135.72, 133.29, 129.87, 129.66, 129.31, 128.96, 128.90, 127.44, 127.17, 122.35, 121.90, 121.28, 116.07, 115.90, 113.54, 99.56, 55.90, 28.06, 25.90, 18.01. ESI-HRMS: ($C_{27}H_{25}FO_3$) calc. [M+H] 417.1867, found 417.1846. General procedure for preparation of aurones derivatives. To a solution of mercuric acetate ($Hg(OAc)_2$) (3 mmol) in DMSO (10 mL) was added 2'-hydroxychalcone (2 mmol) at room temperature and the mixture was stirred at 160 °C for 6 h. The cooled reaction mixture was poured into ice cold water and acidified with 10% aq HCl. The precipitated solid was extracted with dichloromethane or ethyl acetate, the extracts were dried over magnesium sulfate anhydrous and the solvent was evaporated to give a solid which was further purified either by flash column chromatography with *n*-hexane/EtOAc (gradient 20–70% EtOAc) and recrystallisation using absolute EtOH. **(2*Z*)-6-methoxy-2-(*p*-tolylmethylene)benzofuran-3-one (8a)**. Needle-pale yellow crystals, yield 27%, mp 156–157 °C; ^{1}H NMR (500 MHz, $CDCl_3$) δ 7.82 (d, *J* = 8.1 Hz, 2H), 7.73 (d, *J* = 8.5 Hz, 1H), 7.28 (d, *J* = 7.0 Hz, 2H), 6.84 (s, 1H), 6.80 (d, *J* = 2.0 Hz, 1H), 6.78 (dd, *J* = 8.5, 2.1 Hz, 1H), 3.96 (s, 3H), 2.43 (s, 3H). ^{13}C NMR (126 MHz, $CDCl_3$) δ 183.02, 168.47, 167.36, 147.49, 140.11, 131.35, 129.68, 129.64, 125.78, 115.04, 112.15, 112.08, 96.66, 56.01, 21.58. ESI-HRMS: ($C_{17}H_{14}O_3$) calc. [M+H] 267.1022, found 267.1018. **(2*Z*)-2-[(3,4-dimethoxyphenyl)methylene]-6-methoxy-benzofuran-3-one (8b)**. Yellow solid, yield 22%, mp. 186-188 °C; ^{1}H NMR (500 MHz, $CDCl_3$) δ 7.73 (d, *J* = 8.4 Hz, 1H), 7.52 (d, *J* = 1.9 Hz, 1H), 7.49 (dd, *J* = 8.3, 1.9 Hz, 1H), 6.96 (d, *J* = 8.3 Hz, 1H), 6.81 (s, 1H), 6.78 (dd, *J* = 10.5, 2.1 Hz, 2H), 4.00 (s, 3H), 3.96 (s, 3H), 3.95 (s, 3H). ^{13}C NMR (126 MHz, $CDCl_3$) δ 182.94, 168.34, 167.38, 150.84, 149.26, 147.02, 125.91, 125.79, 125.59, 115.31, 113.96, 112.55, 112.15, 111.43, 96.79, 56.17, 56.15, 56.11. ESI-HRMS: ($C_{18}H_{16}O_5$) calc. [M+H] 313.1077, found 313.1098. **(2*Z*)-6-methoxy-5-(3-methylbut-2-enyl)-2-(p-tolylmethylene)benzofuran-3-one (15a)**. Pale yellow solid, yield 33%, mp. 149-150 °C; ^{1}H NMR (500 MHz, $CDCl_3$) δ 7.82 (d, *J* = 8.1 Hz, 2H), 7.57 (s, 1H), 7.27 (d, *J* = 8.1 Hz, 2H), 6.82 (s, 1H), 6.77 (s, 1H), 5.32 (t, 1H), 3.99 (s, 3H), 3.31 (d, *J* = 7.4 Hz, 2H), 2.43 (s, 3H), 1.79 (s, 3H), 1.71 (s, 3H). ^{13}C NMR (126 MHz, $CDCl_3$) δ 167.76, 165.45, 147.79, 140.10, 133.94, 131.45, 129.99, 129.76, 127.16, 124.31, 121.38, 114.23, 111.96, 100.16, 94.40, 56.23, 28.17, 26.00, 21.73, 17.87. ESI-HRMS: ($C_{22}H_{22}O_3$) calc. [M+H] 335.1648, found 335.1654. **(2*Z*)-2-[(3,4-dimethoxyphenyl)methylene]-6-methoxy-5-(3-methylbut-2-enyl)benzofuran-3-one (15b)**. Pale yellow solid, yield 44%, mp 151–152 °C; ^{1}H NMR (500 MHz, $CDCl_3$) δ 7.57 (s, 1H), 7.52 (s, 1H), 7.50 (d, *J* = 8.4 Hz, 1H), 6.96 (d, *J* = 8.4 Hz, 1H), 6.80 (s, 1H), 6.73 (s, 1H), 5.32 (t, 1H), 4.00 (s, 3H), 4.00 (s, 3H), 3.97 (s, 3H), 3.31 (d, *J* = 7.4 Hz, 2H), 1.79 (s, 3H), 1.71 (s, 3H). ^{13}C NMR (126 MHz, $CDCl_3$) δ 183.24, 167.50, 165.33, 150.74, 149.24, 147.16, 133.96, 127.16, 125.75, 125.70, 124.28, 121.36, 114.32, 113.96, 112.19, 111.41, 94.30, 56.24, 56.18, 56.11, 28.16, 26.00, 17.86. ESI-HRMS: ($C_{23}H_{24}O_5$) calc. [M+H] 381.1703, found 381.1703. General procedure for preparation of flavonols derivatives. To a well-stirred solution of 2'-hydroxychalcone derivates (10 mmol) in EtOH (30 mL) and aq KOH (40%, 15 mL), H_2O_2 (30%, 10 mL) was added drop wise for 30 min at room temperature. The reaction mixture was further stirred for 3–4 h. The resulting light-yellow reaction mixture was poured on crushed ice and neutralized with 2 M aq HCl. The light-yellow solid thus obtained was filtered, washed with water and dried. The crude product was purified by flash chromatography with *n*-hexane/EtOAc (gradient 20-70% EtOAc) and recrystallisation using absolute EtOH. **3-hydroxy-7-methoxy-2-*p*-tolyl-4*H*-chromen-4-one (9a)**. Pale brown solid. Yield 43%, mp 220–221 °C; ^{1}H NMR (500 MHz, CDCl3) δ 8.16 (dd, *J* = 8.6, 3.1 Hz, 3H), 7.36 (d, *J* = 8.1 Hz, 2H), 7.02 (dd, *J* = 8.8, 2.2 Hz, 1H), 6.98 (d, *J* = 2.2 Hz, 1H), 3.96 (s, 3H), 2.46 (s, 3H). ^{13}C NMR (126 MHz, $CDCl_3$) δ 164.21, 157.34, 144.61, 140.28, 132.15, 129.32, 128.42, 127.45, 126.74, 114.77, 99.91, 67.84, 55.85, 21.51. ESI-HRMS: ($C_{17}H_{14}O_4$) calc. [M+H] 283.0971, found 283.0970. **2-(3,4-dimethoxyphenyl)-3-hydroxy-7-methoxy-4*H*-chromen-4-one (9b)**. Pale yellow solid, yield 31%, mp 188–189 °C; ^{1}H NMR (500 MHz, $CDCl_3$) δ 8.16 (d, *J* = 8.9 Hz, 1H), 7.88 (dd, *J* = 8.5, 1.9 Hz, 1H), 7.86 (s, *J* = 1.8 Hz, 1H), 7.03 (dd, *J* = 12.5, 5.5 Hz, 2H), 6.98 (d, *J* = 2.2 Hz, 1H), 4.00 (t, 9H). ^{13}C NMR (126 MHz, $CDCl_3$) δ 164.33, 157.36, 150.76, 149.08, 144.65, 132.31, 126.91, 124.09, 121.29, 114.82, 111.17, 110.90, 100.16, 100.11, 68.00, 56.25, 56.14, 56.02. ESI-HRMS: ($C_{18}H_{16}O_6$) calc. [M+H] 329.1026, found 329.1036. General procedure for the preparation of prenylated and geranylated flavonols and aurone derivatives. A mixture of flavonol or aurone derivates (1.5 mmol), 1-chloro-3-methyl-2-butene or geranyl bromide (2 equiv) and anhydrous K_2CO_3 (3 equiv), was stirred in acetone (30 mL) and heated at 75 °C for 20 h. The reaction mixture was monitored by TLC. After completion of the reaction, the reaction mixture was filtrated and evaporated under vacuum. The residue was purified by silica gel flash column chromatography with *n*-hexane/EtOAc (gradient 20-60% EtOAc). **7-methoxy-3-(3-methylbut-2-enyloxy)-2-*p*-tolyl-4*H*-chromen-4-one (10a)**. Pale yellow solid, yield 80%, mp 97–98 °C; ^{1}H NMR (500 MHz, $CDCl_3$) δ 8.17 (d, *J* = 8.9 Hz, 1H), 8.03 (d, *J* = 8.3 Hz, 2H), 7.31 (d, *J* = 8.4 Hz, 2H), 6.97 (dd, *J* = 8.9, 2.3 Hz, 1H), 6.92 (d, *J* = 2.3 Hz, 1H), 5.43 (t, 1H), 4.61 (d, *J* = 7.3 Hz, 2H), 3.93 (s, 3H), 2.45 (s, 3H), 1.69 (s, 3H), 1.64 (s, 3H). ^{13}C NMR (126 MHz, $CDCl_3$) δ 175.24, 164.38, 157.48, 156.29, 141.16, 140.22, 139.52, 129.51, 129.02, 128.93, 127.57, 120.58, 118.58, 114.70, 100.41, 69.18, 56.26, 26.20, 21.97, 18.44. ESI-HRMS: ($C_{22}H_{22}O_4$) calc. [M+H] 351.1597, found 351.1620. **(*E*)-3-(3,7-dimethylocta-2,6-dienyloxy)-7-methoxy-2-*p*-tolyl-4*H*-chromen-4-one (10c)**. Colorless oil, yield 62%; ^{1}H NMR (500 MHz, $CDCl_3$) δ 8.18 (d, *J* = 8.9 Hz, 1H), 8.04 (d, *J* = 8.3 Hz, 2H), 7.31 (d, *J* = 8.1 Hz, 2H), 6.98 (dd, *J* = 8.9, 2.3 Hz, 1H), 6.93 (d, *J* = 2.2 Hz, 1H), 5.42 (t, 1H), 5.06 (t, 1H), 4.66 (d, *J* = 7.2 Hz, 2H), 3.93 (s, 3H), 2.45 (s, 3H), 2.04–1.93 (m, 4H), 1.68–1.54 (m, 9H). ^{13}C NMR (126 MHz, $CDCl_3$) δ 174.80, 163.91, 157.00, 155.80, 142.34, 140.70, 139.73, 131.57, 129.04, 128.56, 128.50, 127.13, 123.96, 119.71, 118.10, 114.24, 99.94, 68.71, 55.80, 39.52, 26.31, 25.63, 21.51, 17.63, 16.43. ESI-HRMS: ($C_{27}H_{30}O_4$) calc. [M+H] 419.2223, found 419.2243. **(E)-2-(3,4-dimethoxyphenyl)-3-(3,7-dimethylocta-2,6-dienyloxy)-7-methoxy-4*H*-chromen-4-one (10d)**. Colorless yellow oil, yield 42%; ^{1}H NMR (500 MHz, CDCl3) δ 8.18 (d, *J* = 8.9 Hz, 1H), 7.85 (d, *J* = 2.0 Hz, 1H), 7.76 (dd, *J* = 8.5, 2.1 Hz, 1H), 7.01–6.97 (m, 2H), 6.93 (d, *J* = 2.3 Hz, 1H), 5.46 (t, 1H), 5.06 (t, 1H), 4.66 (d, *J* = 7.2 Hz, 2H), 3.99 (s, 3H), 3.97 (s, 3H), 3.95 (s, 3H), 2.06–1.94 (m, 4H), 1.67 (s, 3H), 1.63 (s, 3H), 1.58 (s, 3H). ^{13}C NMR (126 MHz, $CDCl_3$) δ 174.82, 164.06, 157.06, 155.52, 151.05, 148.71, 142.44, 139.60, 131.81, 127.32, 124.13, 124.02, 122.04, 119.92, 118.25, 114.28, 112.11, 110.85, 100.15, 68.95, 56.17, 56.11, 55.97, 39.71, 26.49, 25.76, 17.77, 16.61. ESI-HRMS: ($C_{28}H_{32}O_6$) calc. [M+H] 464.2278, found 464.2290.

(b) Representative biological activity procedures. **Cell Culture**. The murine macrophages-like cell line (RAW 264.7) from the European Collection of Cell Cultures (Porton Down, UK) were maintained in DMEM supplemented with 10% FBS, 4.5 g/L glucose, sodium pyruvate (1 mM), L-glutamine (2 mM), streptomycin (50 μg/mL) and penicillin (50 U/mL) at 37 °C and 5% CO_2. When RAW 264.7 cells reached confluences of 80–90%, the cells were scraped out and centrifuged at 110*g* in 4 °C for 10 min. The cell viability of cultured cells used in the assay was always >95% as determined by trypan blue dye exclusion. **Cell Stimulation and Treatment**. RAW 264.7 (4 × 105 cells/well) were seeded into a tissue culture grade 96-well plate except for blank and incubated for 2 h at 37 °C, 5% CO_2 for cell attachment. The attached cells were activated with 100 U/mL of recombinant IFN-γ and 5 μg/mL of LPS with or without presence of synthetic compound at a final volume of 100 μL/well. DMSO was used as vehicle to add synthetic compound into the culture medium and the final concentration of DMSO was 0.1% in all cultures. Cells were then incubated at 37 °C, 5% CO_2 for 17–20 h. The level of PGE2 was determined by using PGE2 EIA kit (Item No. 500141). **Cell Viability**. The cytotoxicity of synthetic compound on cultured cells was determined by assaying the reduction of MTT reagents to formazan salts. After treatment, the supernatant of 96-wells plate containing cells were removed and MTT reagents (0.05 mg/mL) were added into each well. The cells were incubated in 37 °C for 4 h and the formazan salts were dissolved by adding 100% DMSO. The absorbance was then measured at 570 nm on a SpectraMax Plus microplate reader (Molecular Devices Inc., Sunnyvale, CA, USA). **Determination of PGE_2**. The cell culture supernatants were collected and analyzed for PGE_2 secretion PGE_2 EIA kits (Cayman Chemical, Ann Arbor, MI, USA). The protocols provided by the manufacturers were followed to the detail. The data was acquired using a SpectraMax Plus microplate reader (Molecular Device, Sunnyvale, CA, USA). The concentration of PGE_2 for each sample was calculated from their respective standard curves.

(c) X-ray structure determination. Single crystal X-ray experiment of **14b** was performed on Bruker D-QUEST diffractometer using graphite-monochromated Mo-Kα radiation (λ = 0.71073 Å). Intensity data was measured at 301(2)°K by the ω-scan. Accurate cell parameters and orientation matrix were determined by the least-squares fit of 25 reflections. Intensity data was collected for Lorentz and polarization effects. Empirical absorption correction was carried out using multi-scan. The structure was solved by direct methods and least-squares refinement of the structure was performed by the SHELXL-97 program. All the non-hydrogen atoms were refined anisotropically. The hydrogen atoms were placed in calculated positions, allowing them to ride on their parent C atom with $Uiso(H) = xU_{eq}(C)$ where, *x* = 1.5 for methyl; 1.2 for non-methyl groups, except the hydrogen atoms attached to oxygen atoms were located from Fourier maps and refined isotropically. A summary of the data collections and details of the structure refinement is given in Tables 2 and 3. Crystallographic data for the structural determination has been deposited with the Cambridge Crystallographic Data Centre, CCDC No **997318**. This information may be obtained free of charge from the Director, CCDC, 12 Union Road, Cambridge CB2, 1EZ, UK; http://www.ccdccam.ac.uk/const/retrieving.html).

(d) Molecular Modeling. All molecular modeling methods were performed using Discovery Studio 3.1 (Accelrys, San Diego, USA) on an Intel® (TM)2 Quad CPU Q8200 @2.33 GHz running under a Windows XP Professional environment.

20. Sugamoto, K.; Matsusita, Y.-I.; Matsui, K.; Kurogi, C.; Matsui, T. *Tetrahedron* **2011**, *67*, 5346.
21. Dong, X.; Qi, L.; Jiang, C.; Chen, J.; Wei, E.; Hu, Y. *Bioorg. Med. Chem. Lett.* **2009**, *19*, 3196.
22. Chu, W. L. A.; Jensen, F. R.; Jensen, T. B.; McAlpine, J. B.; Søkilde, B.; SantAna-Sørensen, A. M.; Ratnayake, S.; Jiang, J. B.; Noble, C.; Stafford, A. M.; Google Patents: **2001**.
23. Suzuki, A. *Angew. Chem., Int. Ed.* **2011**, *50*, 6722.
24. Han, W.; Liu, C.; Jin, Z.-L. *Org. Lett.* **2007**, *9*, 4005.
25. Sjögren, T.; Nord, J.; Ek, M.; Johansson, P.; Liu, G.; Geschwindner, S. *Proc. Natl. Acad. Sci.* **2013**, *110*, 3806.
26. Kurumbail, R. G.; Stevens, A. M.; Gierse, J. K.; McDonald, J. J.; Stegeman, R. A.; Pak, J. Y.; Gildehaus, D.; Iyashiro, J. M.; Penning, T. D.; Seibert, K.; Isakson, P. C.; Stallings, W. C. *Nature* **1996**, *384*, 644.
27. Wang, J. L.; Limburg, D.; Graneto, M. J.; Springer, J.; Hamper, J. R. B.; Liao, S.; Pawlitz, J. L.; Kurumbail, R. G.; Maziasz, T.; Talley, J. J.; Kiefer, J. R.; Carter, J. *Bioorg. Med. Chem. Lett.* **2010**, *20*, 7159.
28. Garavito, R. M.; DeWitt, D. L. *Biochimica et Biophysica Acta (BBA)-Mol. Cell Biol. Lipids* **1999**, *1441*, 278.